FOCUS: EMERGING INVESTIGATORS: RESEARCH ARTICLE

Tapered-Tip Capillary Electrophoresis Nano-Electrospray Ionization Mass Spectrometry for Ultrasensitive Proteomics: the Mouse Cortex

Sam B. Choi,[1] Marta Zamarbide,[2] M. Chiara Manzini,[2] Peter Nemes[1]

[1]Department of Chemistry, The George Washington University, Washington, DC 20052, USA
[2]Department of Pharmacology and Physiology, The George Washington University, Washington, DC 20037, USA
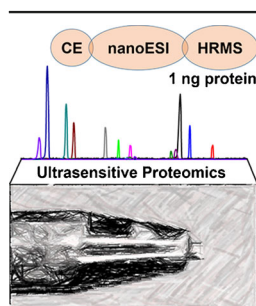
Abstract. Ultrasensitive characterization of the proteome raises the potential to understand how differential gene expression orchestrates cell heterogeneity in the brain. Here, we report a microanalytical capillary electrophoresis nano-flow electrospray ionization (CE-nanoESI) interface for mass spectrometry to enable the measurement of limited amounts of proteins in the mouse cortex. Our design integrates a custom-built CE system to a tapered-tip metal emitter in a co-axial sheath-flow configuration. This interface can be constructed in <15 min using readily available components, facilitating broad adaptation. Tapered-tip CE-nanoESI generates stable electrospray by reproducibly anchoring the Taylor cone, minimizes sample dilution in the ion source, and ensures efficient ion generation by sustaining the cone-jet spraying regime. Parallel reaction monitoring provided a 260-zmol lower limit of detection for angiotensin II (156,000 copies). CE was able to resolve a complex mixture of peptides in ~330,000 theoretical plates and identify ~15 amol (~1 pg) of BSA or cytochrome *c*. Over 30 min of separation, 1 ng protein digest from the mouse cortex yielded 217 nonredundant proteins encompassing a ~3-log-order concentration range using a quadrupole time-of-flight mass spectrometer. Identified proteins included many products from genes that are traditionally used to mark oligodendrocytes, astrocytes, and microglia. Finally, key proteins involved in neurodegenerative disorders were detected (e.g., parkinsonism and spastic paraplegia). CE-nanoESI-HRMS delivers sufficient sensitivity to detect proteins in limited amounts of tissues and cell populations to help understand how gene expression differences maintain cell heterogeneity in the brain.

Keywords: Capillary electrophoresis, Mass spectrometry, Bottom-up proteomics, Neuron, Central nervous system, Mouse

Introduction

Unbiased characterization of gene expression has the potential to reveal how the central nervous system establishes enormous cell and tissue diversity. Starting with usually thousands–millions of cells, high-resolution mass spectrometry (HRMS) is able to characterize the encoded proteome and quantify translational and post-translational modifications [1–4].

The mass spectrometry proteomics data have been deposited to the ProteomeXchange Consortium via the PRIDE [69] partner repository with the dataset identifier PXD005222.

Electronic supplementary material The online version of this article (doi:10. 1007/s13361-016-1532-8) contains supplementary material, which is available to authorized users.

Correspondence to: Peter Nemes; *e-mail:* petern@gwu.edu

Discovery HRMS enabled drafting of the human proteome [5] and, recently, cataloging gene expression diversity between tissues and cell types in the mouse brain [6], complementing cell heterogeneity information at the transcriptomic level [7, 8]. Extension of proteomics to small populations of neurons would empower brain research, but this requires new microanalytical HRMS solutions capable of measuring trace amounts of proteins.

There have been a handful of reports on proteomics from nanograms–subnanograms of proteins (see recent reviews including references [9–12]). Single-cell HRMS was pioneered with the detection of 450 amol (~10 ng) α- and β-globulins from human erythrocytes [13] and carbonic anhydrase [14] in diluted lysates by capillary electrophoresis (CE) Fourier transform ion cyclotron resonance (FTICR). For targeted proteins, gains in detection sensitivity and throughput were possible using microfluidics (two proteins with 12 cells/s) [15] and mass

cytometry (34 proteins with 1000 cells/s) [16]. In parallel, refinements in sample preparation and nano-flow liquid chromatography (nanoLC) HRMS extended mass-limited proteomics to discovery operation. Representative cases include identification of 2000 proteins from <400 ng proteins from Langerhans islets [17], 145–187 proteins from 500 breast cancer cells (~150 ng protein) [18], and 109 proteins from 100 HeLa cells [19]. Additionally, porous layer open tubular (PLOT) columns yielded 566 proteins from 50 ng *M. acetivorans* [20] and 163 proteins from ~20 cervical cancer cells (~2.5 ng) [21]. Using FTICR, 870 proteins were identified from 50 ng proteins from *D. radiodurans* with an estimated 7 amol lower limit of detection [22]. Most recently, 1327 proteins were identified from 50 human breast adenocarcinoma cells (~5 ng protein) using focused acoustics-assisted sample preparation and 4-h-long separation on a PLOT column [23]. These examples demonstrate substantial sensitivity improvements in nano-flow LC to extend proteomics to limited samples.

CE is an alternative technology with orthogonal advantages for trace amounts of proteins. High separation power, compatibility with limited samples, fast separation (<1 h), and remarkable limits of detection were demonstrated early by a coaxial sheath-flow electrospray ionization (ESI) interface supplemented with a nebulizer gas [24]. Since this milestone work, various CE-ESI designs were developed in pursuit of sensitivity and robustness (see reviews elsewhere [25–27]). To enhance sensitivity, one group of interfaces eliminates the sheath liquid ("sheathless" designs) to avoid sample dilution in the ion source and maintains nano-flow electrospray ionization (nanoESI) through pulled and/or coated capillaries [28–32]. Emitter clogging and loss of electrical contact have been reported to affect the operational durability of these devices. The porous-junction interface [33] enhanced robustness and sensitivity to 30 amol lower limit of detection for peptides and protein standards [34, 35], detecting 385 proteins from 5 ng digest of the extremophile *P. furiosus* [36] in a bottom-up strategy. Most recently, 5-amol detection was accomplished for targeted peptides by directly hyphenating a CE capillary to an ESI emitter [37]. Sheathless interfaces have also demonstrated utility for intact proteins from a few hundred nanograms of proteins [38–40].

"Sheath-flow" CE-ESI devices are attractive due to easier construction, enhanced robustness, and compatibility with different modalities of CE separation. The broadly successful sheath-flow design [24] surrounds the CE capillary with a sheath liquid at tens of μL/min to complete the electrical circuit [41] and a stream of concentric, heated nebulization gas (L/min) to facilitate droplet desolvation. CE-ESI sensitivity was improved by eliminating the nebulizer gas and lowering the sheath liquid rate to 5–10 μL/min [42]. Further reduction of the sheath liquid rate using an electrokinetic pump and integration of the CE capillary into a pulled nanoESI emitter achieved ~335–600 zmol lower limit of detection for protein standards via multiple reaction monitoring [43, 44]. Furthermore, refinement to this interface yielded an estimated 1 zmol lower limit of detection on a hybrid quadrupole Orbitrap mass spectrometer,

enabling the identification of 60 proteins from 400 fg digest from *E. coli* [45] in a bottom-up and 30 proteins from *P. aeruginosa* in a top-down approach [46]. Most recently, 1249 different proteins were identified from 300 ng digest from the *Xenopus laevis* fertilized egg [47] and 2313 phosphorylated peptides in 200 ng protein from human mammary cells [48] in discovery MS. The electrokinetically pumped CE-nanoESI interface achieves ultrasensitive operation but requires specialized expertise, including HF etching, to assemble the ionization source. The recent commercialization of this interface alleviates some of these challenges.

Over the last 6 y, we and others have designed readily constructible, low-cost sheath-flow CE-ESI interfaces for trace-level measurements. Our designs eliminated the nebulizer gas and used blunt-tip metal emitters (260/130 μm o.d./i.d.) to sustain the sheath liquid at 700–1000 nL/min in the stable cone-jet regime to ensure efficient ion generation. CE-micro-flow ESI (μESI) enabled lower limits of detection at 10–50 nM, or 60–300 amol, for metabolites [49–54] and 3.5–11 nM, or 25–75-amol, for peptides [55, 56]. Large-bore emitters (e.g., 720/420 μm o.d./i.d.) were recently found to compromise the sensitivity of this design to 100 nM, or ~1 fmol limit of detection [57], underscoring that the geometry of the emitter has important impacts on sensitivity. Our CE-μESI interfaces enabled the identification of ~1700 and quantification of 500–800 proteins in 10 ng protein digest from single embryonic cells in the 16-cell *Xenopus laevis* embryo, marking the first time metabolomics and proteomics was performed in actual single cells in the cleavage-stage (16-cell) *Xenopus* embryo [55, 56].

Here, we report a readily constructible sheath-flow CE-ESI design that is able to operate in the nano-flow regime to enable ultrasensitive bottom-up proteomics of the mouse cortex. We extended CE-μESI into the nano-flow regime (~100–300 nL/min sheath) and selected a tapered-tip metal emitter to serve as the sheath supply and ESI source. Peptide separation and quantification were reproducible across several weeks with a lower limit of detection estimated at 260 zmol for angiotensin II (156,000 copies) in parallel reaction monitoring. Identification of model proteins from ~1 pg amount demonstrated ultrasensitive detection. A 1 ng protein digest from the mouse cortex yielded 217 different protein groups using a quadrupole time-of-flight mass spectrometer. CE-identified proteins included products from many genes that mark major cell types in the brain, ranging from neurons to oligodendrocytes, astrocytes, and microglia. Ultrasensitive proteomics by CE-nanoESI-MS raises a potential to characterize gene translation in small populations of cells or single cells to help understand cell heterogeneity during normal brain function and disease.

Experimental

Materials

All materials were purchased at reagent grade or higher from Sigma-Aldrich (St. Louis, MO, USA) unless noted otherwise. Sodium dodecyl sulfate (SDS) was from Amresco (Solon, OH, USA). Reagent-grade ethylenediamine tetraacetic acid

(EDTA), MS-grade trypsin protease, and LC-MS grade aceto-nitrile (ACN), methanol (MeOH), formic acid (FA), and water (Optima) were from Fisher Scientific (Fair Lawn, NJ, USA). All standards were prepared in 500-µL or 2-mL LoBind protein microtubes from Eppendorf (Hauppauge, NY, USA).

Buffers and Standard Solutions

The lysis buffer was prepared to contain: 20 mM Tris–HCl, 5 mM EDTA, 1% (v/v) SDS, and 35 mM NaCl. Peptide standards were serially diluted from a 200 ng/µL stock (in deionized water) using 25% (v/v) ACN containing 0.05% (v/v) FA. Standard bovine serum albumin (BSA, 1 µg/µL) in TEAB buffer (100 mM) was reduced with dithiothreitol (1 M), alkylated with iodoacetamide (1 M), and digested with trypsin [enzyme:protein = 1:50 (w/w)] over 12 h at 37 °C. The digest was lyophilized and reconstituted at 2 µg/µL in 75% (v/v) ACN containing 0.05% (v/v) FA before serial dilution using the same solvent. Solutions were vortex-mixed, centrifuged at $10,000 \times g$ for 60 s at 4 °C, and stored at −20 °C until measurement by CE-nanoESI-HRMS. The background electrolyte (BGE) consisted of 50% ACN with 1 M FA (yielding pH 2.3).

Animals

All procedures regarding the maintenance and humane treatment of mice were authorized by the George Washington University Institutional Animal Care and Use Committee (IACUC Approval Number A274). Adult male mice (Mus musculus) were purchased from Charles River Laboratories (Wilmington, MA, USA) and maintained in a breeding colony. Four-month-old adult male mice were sacrificed by cervical dislocation. The brain was surgically removed, placed on ice, and rinsed with ice-cold phosphate buffer solution to remove residual blood and contaminants. The posterior half of the cortex was identified in reference to the Allan Brain Atlas, and the tissue was dissected and immediately frozen in liquid nitrogen. The sample was stored at −80 °C until analysis within a month.

Proteomic Sample Preparation

The dissected tissue was lysed in 500 µL lysis buffer, facilitated by sonication for 15 min in water bath (~4 °C). The lysate was reduced (5 µL of 1 M dithiothreitol, 30 min at 60 °C) and alkylated (10 µL of 1 M iodoacetamide, 15 min in the dark) before quenching the reaction (5 µL of dithiothreitol). To remove cell debris, the lysate was centrifuged at $11,200 \times g$ for 10 min at 4 °C, and the supernatant was aliquoted into a separate LoBind microtube. Proteins in the aliquot were purified by precipitation over 12 h in 2 mL of chilled acetone (−20 °C), followed by centrifugation at $11,200 \times g$ for 10 min at 4 °C. The protein pellet was washed with chilled acetone, lyophilized at room temperature, and reconstituted to 1 µg/µL protein concentration in 500 µL of ammonium bicarbonate (50 mM) based on the standard bicinchoninic acid (BCA) assay (Thermo Scientific, Waltham, MA, USA). Aliquots of 50 µL were separated into individual LoBind microtubes to serve as

technical replicates. Each aliquot was digested with 1 µL of trypsin (1 mg/mL) over 12 h at 37 °C. The digests were lyophilized and suspended in 50 µL of 50% (v/v) ACN containing 0.05% (v/v) AcOH, which was selected to enable on-column preconcentration by field-amplified sample stacking in a higher-conductivity BGE during measurement by CE-HRMS.

CE-nanoESI-MS

The microanalytical CE platform was constructed based on our recent prototypes [51, 53, 55] and operated for bottom-up proteomics as described elsewhere [55, 56]. During sample loading, a 1 µL portion of the sample was deposited into a microloading vial, whence 1 nL (~1 ng protein digest) was hydrodynamically injected into the CE separation capillary (90/20 µm o.d./i.d., 90 cm length) by elevating the capillary inlet 20 cm above the outlet end for 3 min. Peptides were separated by applying 22–26 kV to the capillary inlet. The CE electrical circuit was completed through a sheath solution (50% MeOH in 0.1% FA), which was fed through a grounded metal emitter and supplied by a low-flow syringe pump (model Pico Plus Elite; Harvard Apparatus, Holliston, MA, USA).

The CE-nanoESI interface was built from commercially available parts. The following components were used in the construction (part number, p/n): fused silica capillary for electrospray sheath (360/75 µm o.d./i.d., p/n #106815-0019; Polymicro Technologies, Phoenix, AZ, USA) and for CE separation (90/20 µm o.d./i.d., p/n #106815-0381; Polymicro); metal tapered-tip emitter for nanoelectrospray (320/100 µm o.d./i.d., p/n MT320-100-3.5-5, New Objective, Woburn, MA, USA); sleeves to mount sheath flow (p/n F-172; IDEX Health and Science, Oak Harbor, WA, USA), and CE (p/n F-180x; IDEX) capillary; T-union to mount parts (MicroTee, p/n P-888; IDEX). The CE-nanoESI interface was mounted on a three-axis translation stage to align the emitter tip with the orifice of a mass spectrometer. The Taylor cone was monitored using a long-working distance objective (Plan APO, 20× 0.42 NA, Mitutoyo America Corp., Aurora, IL, USA) and a CCD camera (EO-2018C; from Edmund Optics Inc., Barrington, NJ, USA). The stability of ion generation was evaluated based on the ion signal recorded by a mass spectrometer.

Peptide ions were mass-analyzed between m/z 350 and 2400 by a quadrupole orthogonal acceleration time-of-flight mass spectrometer equipped with a collision-induced dissociation (CID) cell (Qq-TOF, Impact HD; Bruker Daltonics, Billerica, MA, USA). The mass spectrometer was tuned and calibrated according to vendor specifications and operated at 40,000 FWHM resolution. To identify peptides, signals were fragmented via data-dependent acquisition (DDA) with the following settings: data acquisition rate, 4 Hz for MS^1 and 1 Hz for MS^2; survey scan interval, 3 s; fragmentation preference, top most-intense; MS^2 threshold, 500 counts per 1000 summations; mass accuracy for dynamic exclusion, 50 mDa; m/z window and CID energy, 8 Da and 20–70 eV depending on

charge state; collision gas, nitrogen; and dynamic exclusion, applied; smart exclusion, applied with 5× threshold.

Data Analysis

Peptide standards were quantified based on area-under-the-curve in selected-ion electropherograms that were generated with 10 mDa window in DataAnalysis. For the standard BSA and cytochrome *c*, primary MS-MS/MS data were exported into XML in DataAnalysis 4.3 (Bruker Daltonics) and processed in ProteinScape 3.1 using Mascot 2.5.1 search engine. The data were searched against the SwissProt Mammalian proteome database (downloaded on December 15, 2015). The search parameters were: digestion, tryptic; missed cleavages, maximum 2; minimum number of unique peptides, 1; MS/MS score threshold, 4.5; fixed modification, carbamidomethylation at cysteine; variable modification, oxidation at methionine; and MS tolerance for peptides and fragments, ±20 ppm and ±0.1 Da, respectively. For the mouse brain tissue, the raw mass spectrometric data were analyzed with MaxQuant 1.5.3.30 (Max Planck Institute of Biochemistry) executing Andromeda 1.5.3.8 search engine. The MS-MS/MS data were searched against the SwissProt mouse (*Mus musculus*) proteome database (downloaded from UniProt on November 11, 2015) containing 16,792 entries, as well as contaminants from the common Repository of Adventitious Proteins (cRAP) database (downloaded from the Global Proteome Machine [58] on July 28, 2016) containing 115 entries. The search parameters were identical as earlier, except for the following instrument-specific parameters: main search peptide tolerance, 6 mDa; TOF MS/MS match tolerance, 30 ppm; isotope match tolerance, 5 mDa; decoy mode, revert. Proteins were identified based on at least one sequence-unique peptide match (see sequence annotations in the Supporting Information document) with false discovery rate (FDR) <1% against a reversed-sequence decoy database. Proteins are reported as protein groups based on the closest parsimony principle. Common contaminant proteins were removed from the list of proteins reported in this work.

Safety Considerations

Standard safety protocols were followed when working with chemicals. Capillaries pose poking hazard and were handled with care. All conductive parts of the CE-nanoESI system were shielded or grounded to prevent accidental exposure.

Results and Discussion

The overall goal of this study was to develop a microanalytical HRMS that enables the discovery characterization of protein amounts contained in limited cortical tissues, particularly small populations of neurons. Our experiments based on cultured cortical neurons and a total protein assay (BCA) found that 5–50-μm-diameter neurons contain <500 pg of total protein. Therefore, a handful of neurons are estimated to contain ~1 ng

total protein. As this protein amount is ~1000–10,000-times smaller than common to nanoLC-nanoESI-HRMS analyses, the technology of choice in discovery proteomics, our goal necessitated the development of an alternative approach. One such technology is CE-HRMS, which is compatible with samples limited to ~1–100 nL, provides exquisite peak capacity, and can be coupled to HRMS [59]. Indeed, a microanalytical CE-μESI-HRMS platform that we recently built was capable of detecting 1709 and quantifying hundreds of proteins in ~20 ng protein digests from single embryonic cells of *Xenopus laevis* [55, 56]. However, as protein amounts contained in a handful of neurons to single neurons are 20–100-times smaller, our goal required significant advances in the sensitivity of CE-ESI-HRMS.

To bridge this technological gap, we here advanced CE-ESI-HRMS sensitivity to enable bottom-up proteomics from ~1 ng protein digest. Our approach (Fig. 1) used diluted protein digests from the mouse brain to aid technology development
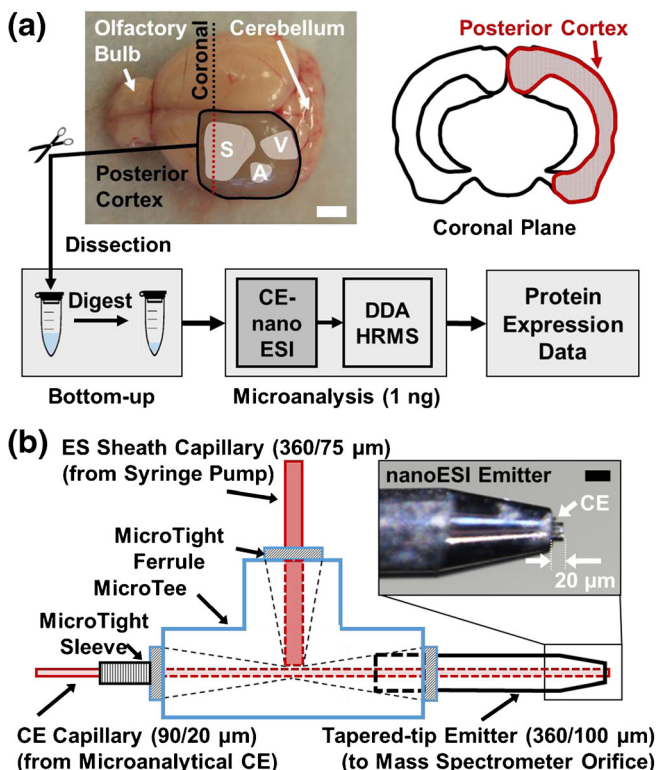
Figure 1. The proposed microanalytical methodology for trace-level proteomics in the mouse brain. (**a**) The posterior half of the mouse cortex was identified and dissected free of underlying tissues (see highlight and coronal section). For reference, location of the somatosensory (S), visual (V), and auditory (A) structures are highlighted. Proteins were processed via a bottom-up workflow and the resulting peptides measured. (**b**) Schematics of the tapered-tip capillary electrophoresis (CE) nanoelectrospray ionization (nanoESI) interface for ultrasensitive proteomics. The interface used readily available commercial parts to facilitate broad adoption (see vendor and parts information in the Methods). Scale bar = 2 mm (white), 100 μm (black)

and validation. In this study, the posterior half of the mouse cortex (Fig. 1a), which includes the occipital, temporal, and parietal cortical regions, was selected as the model, although any regions of the brain, tissues, or limited populations of cells should be amenable to the workflow. The cortical tissue was dissected, and the proteins were extracted, reduced, alkylated, and trypsin-digested using a standard bottom-up proteomic workflow (see Methods). The resulting digest was diluted to 1 ng/nL concentration, and a volume containing 1 ng protein digest (1 nL) was used to approximate the total protein content of a handful of mammalian neurons in this study.

Initially, we tested our sheath-flow CE-µESI interface for measuring this limited protein digest. Based on earlier designs [49, 51, 55, 56], we constructed a microsampling stage capable of reproducibly loading 1 nL, or ~1 ng protein digest into a CE capillary (see Methods for details). The capillary was connected to a CE-µESI interface, which featured a 260/133 µm o.d./i.d. blunt-tip stainless steel tubing (Hamilton Company, Reno, NV, USA). As ESI efficiency depends on electrosprayed droplet size [41] and droplet size varies with flow rate [41], we proposed that further sensitivity enhancements are possible using this CE-µESI device by lowering the sheath liquid rate to the nano-flow regime. The scaling laws of electrospray [60] suggest that transitioning from 1 µL/min to ~200–300 nL/min sheath rate, which is the flow rate domain in standard nanoLC-nanoESI-MS, reduces electrosprayed droplet size by 50%. However, our tests showed that the electrospray was unstable below ~500 nL/min sheath liquid: the ion current was frequented by low-intensity domains and current spikes. Microscopy of the electrified meniscus captured transitions from the cone-jet regime to the non-axial (multijet) and pulsating (burst or astable) spraying modes. Additionally, the electrified liquid meniscus was ill-anchored on the rim of the emitter with frequent transitions between the outer and the inner edges of the rim, likely causing unstable droplet trajectories toward the MS orifice. As these factors combined lowered sensitivity, our goals necessitated an alternative sheath-flow design to measure the limited protein digests.

These observations guided the design of a new CE-ESI interface capable of stable operation in the nano-flow regime (CE-nanoESI) for efficient ion generation. The co-axial sheath-flow configuration was selected because of its robust operation and compatibility with diverse CE separation modes. An additional consideration was the use of readily available commercial parts and a simplified configuration to aid instrument construction and transferability to other laboratories. To help reproducibly anchor the Taylor cone, we evaluated metal blunt-tip emitters (Hamilton) with narrower rim dimensions than earlier as well as emitters with tapered-tip geometry (New Objective) that essentially eliminates the rim. Using a T-union, the CE fused silica separation capillary (90/20 µm o.d./i.d.) was mounted into blunt tip metal emitters with 210/108 µm (gauge 33) or 235/108 µm o.d./i.d. (gauge 32) or emitters tapered to 100 µm o.d./i.d. (New Objective). The CE capillary was adjusted to protrude 10–20 µm from the emitter tip to minimize sample dilution in the ion source (see tapered-tip design in

Figure 1b). These CE-ESI constructs were installed in front of a mass spectrometer, and stability of the Taylor cone was imaged in ESI-only (CE turned off) and CE-ESI operation (CE on) using a long-distance microscope (data not shown). At 200–350 nL/min sheath liquid, the tapered-tip design anchored the Taylor cone most stably and produced the most stable ion current, ensuring robust nanoESI for several hours of tested operation.

Therefore, this tapered-tip CE-nanoESI interface was selected for further characterization as an ionization source. Ideally, the ion source is operated in the cone-jet regime, which is the most efficient for ion generation [61, 62]. To enhance ionization efficiency, angiotensin II was supplied at 100 nM in 50% MeOH, 0.1% FA through the sheath liquid using a syringe pump, and a long working-distance camera was used to position the CE-nanoESI emitter in front of the mass spectrometer orifice plate to establish the cone-jet regime. The mass spectrometer was used to evaluate the ion yields as a function of emitter-to-mass spectrometer orifice distance (d_{ES-OR}), electrospray potential, and sheath flow rate. Figure 2a maps the onset and stability domains of the cone-jet regime. Shorter distances yielded significantly higher ion currents and better spray stability (less error) for the peptide, which we ascribe to more efficient entraining of electrosprayed droplets into the mass spectrometer. These data suggest further sensitivity enhancements possible with shorter distances; however, electric discharge (corona discharge, sparks, or arc) presents a practical boundary condition at ~300 µm distance from the MS orifice using the current emitter material. Nonconductive emitters, similar to pulled borosilicate [47] or fused silica capillaries, may help reduce d_{ES-OR} in the presented sheath-flow configuration. Afterward, the rate of sheath flow was refined using a mixture of standard peptides in the CE-nanoESI modality (Figure 2b). Angiotensin II, leucine enkephalin, and methionine enkephalin were detected in the highest ion signal intensity (electrophoretic peak area) at 300 nL/min sheath, which corresponds to the flow rate domain used in standard nanoLC-nanoESI-HRMS.

Next, the interface was evaluated for electrophoretically separating the peptide standards as model for a bottom-up proteomic workflow (Figure 3a). Without Joule heating or electrolysis, the CE current is expected to correlate linearly with the applied potential (Ohm's law). Indeed, a broad range of separation potentials ensured Ohmic characteristics with a ~7.64 ± 0.06 MΩ net resistance for the CE circuit. A more than 3% deviation from the expected CE current versus voltage correlation was selected to mark the upper limit of the dynamic range of separation potential above ~27 kV. Although higher separation voltage provided faster separation, lower CE voltages were advantageous for resolving co-migrating species. For example, the peak-to-peak resolution between the Leu-Enk and Met-Enk improved from 1.13 at 27 kV and 1.35 at 25 kV to 1.61 at 23 kV CE potential, as moderately lower potentials provided slightly longer times for separation to unfold (without causing detectable peak broadening due to diffusion). A stable total ion current signal over an extended period,
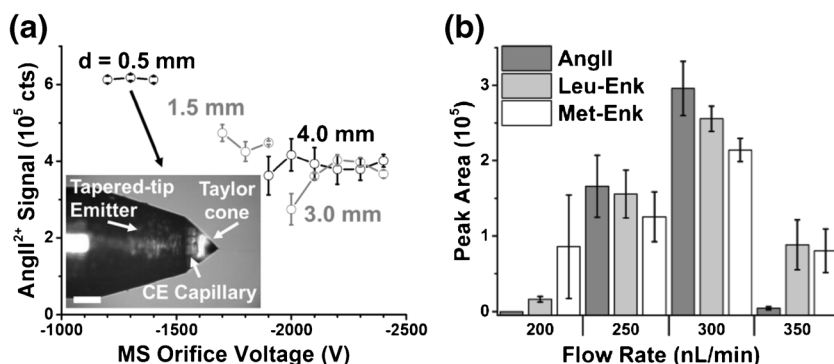
Figure 2. Configuration of ionization sensitivity. The CE-nanoESI sheath liquid contained angiotensin II (AngII) to quantify detection sensitivity as a function of spray-to-MS orifice distance ($d_{ES\text{-}OR}$), electrospray potential, and sheath supply rate. (**a**) On-set and stability domains of the cone-jet spraying regime at 300 nL/min sheath without CE (CE voltage turned off). The inset shows stable anchoring of the Taylor cone at the tapered-tip emitter and the CE separation capillary protruding ~10–20 μm into the Taylor cone. Scale bar = 50 μm. (**b**) Angiotensin II, leucine enkephalin (Leu-Enk), and methionine enkephalin (Met-Enk) were detected in the highest signal abundance at 300 nL/min sheath rate. Therefore, the final experimental settings in this study were: $d_{ES\text{-}OR}$ = 0.5 mm, electrospray potential = –1300 V on MS sampling plate (versus grounded electrospray emitter). Error bars show S.E.M

~90 min (see TIC in inset), confirmed robust CE-nanoESI operation. Technical quadruplet analysis of the angiotensin II standard revealed that the same-day repeatability was ~2% relative standard deviation (RSD) in migration time and ~20% RSD in quantification based on under-the-peak-areas calculated in selected-ion electropherograms. Angiotensin II was separated with a theoretical plate number of ~330,000 in BGE prepared with 1 M FA. These analytical figures of metrics raised a potential to address complex protein digests.

Detection sensitivity was tested using serial dilutions. Based on under-the-peak-areas in selected ion electropherograms, the peptide mix was quantified over a 4-log-order dynamic range

(Figure 3b). Two amol of angiotensin II yielded S/N = 17.0 (signal height/noise root mean square) in single-stage (MS^1) modality, which extrapolates to ~350-zmol (~210,000 copies) peptide in a discovery (untargeted) approach at S/N = 3. This sensitivity is ~70-fold higher compared with our previous blunt-tip CE-μESI design [55, 56]. To directly compare the sensitivity of these nano- and micro-flow CE-ESI designs under identical experimental conditions, we established stable cone-jet spraying regime for the tapered-tip CE-nanoESI and the blunt-tip CE-μESI interfaces and performed parallel reaction monitoring (PRM) for AngII^{2+} using the same mass spectrometer and data acquisition settings (see Methods).
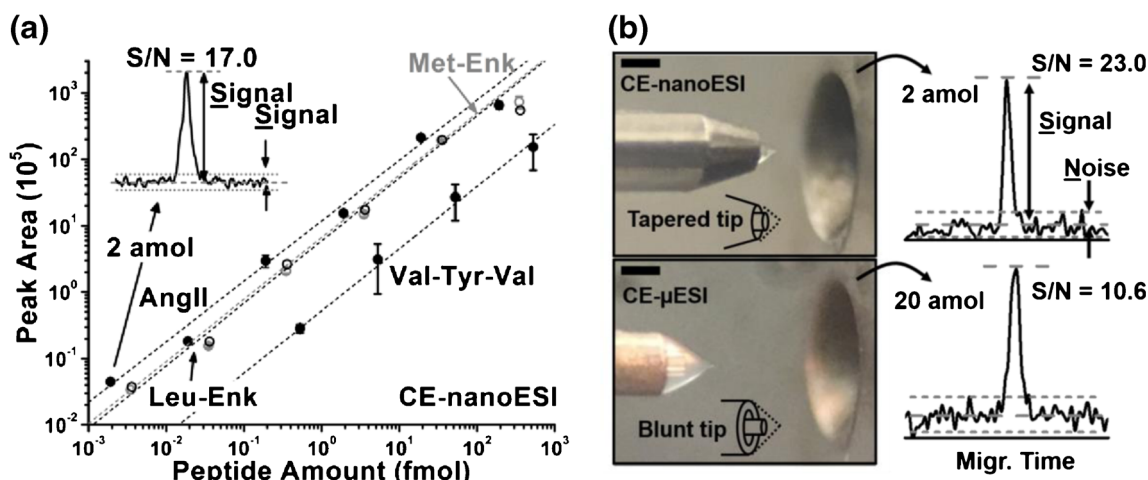

Figure 3. Ultra-sensitive peptide detection. (**a**) CE-nanoESI-HRM separated angiotensin II (AngII), leucine enkephalin (Leu-Enk), methionine enkephalin (Met-Enk), and valine-tyrosine-valine (Val-Tyr-Val) in high efficiency (330,000 theoretical plates for angiotensin II). Quantification was linear over a 4–5 log-order concentration range (R^2 > 0.9 for each different peptide) using single-stage MS. Error bars show S.E.M. (**b**) Sensitivity of CE tapered-tip nanoESI (**top panels**) was evaluated and compared with our earlier blunt-tip CE-μESI (**bottom panels**) interface. Optical imaging revealed that the tapered-tip geometry sustained a smaller Taylor cone with stable anchoring on the emitter rim, enabling robust operation (see top panel). Parallel reaction monitoring of the y_2 fragment from angiotensin II indicated a ~260-zmol lower limit of detection (156,000 copies) for the peptide using the tapered-tip versus ~5 amol by the blunt-tip. These results confirmed ultrasensitive detection by CE-nanoESI-HRMS. Scale bars = 150 μm. Experimental conditions: $d_{ES\text{-}OR}$ = ~500 μm, –1300 V spray, 25 kV separation for CE-nanoESI; $d_{ES\text{-}OR}$ = ~1.5 mm, –1700 V spray, 27 kV separation for CE-μESI

Microscopy imaging revealed (see Figure 3b) that CE-nanoESI sustained a Taylor cone of ~100 fL at 300 nL/min sheath, whereas the liquid cone in the blunt-tip design (260/130 µm o.d./i.d.) measured ~5 nL at 1 µL/min sheath. Additionally, the CE-µESI interface required larger distance from the orifice of the mass spectrometer to maintain the cone-jet regime (Figure 3b). Therefore, tapered-tip CE-nanoESI was anticipated to cause less dilution for peptides migrating into the Taylor cone and also ensure more efficient ion transfer into the mass spectrometer. With the CE-nanoESI interface, targeted MS/MS on 2 amol of $AngII^{2+}$ generated the b_2^+, b_4^+, and b_6^+ fragments in detectable signal intensity (S/N > 3) and the y_2^+ fragment in high abundance, essentially identifying the peptide sequence (data not shown). A 2 amol of $AngII^{2+}$ yielded the y_2^+ fragment at S/N = 23 in the corresponding selected-ion electropherogram, indicating a 260-zmol lower limit of detection, or 156,000 copies of the peptide. In comparison 20 amol $AngII^{2+}$ yielded S/N = 10.6, suggesting an ~6 amol lower limit of detection using CE-µESI. Therefore, the tapered-tip design provided a 22-fold sensitivity improvement compared to CE-µESI interface, raising a potential for ultrasensitive proteomics.

Mass-Limited Protein Digests

Tapered-tip CE-nanoESI-MS was tested for trace amounts of proteins. Digests of standard BSA and cytochrome *c* were serially diluted in 75% (v/v) ACN containing 0.05% (v/v) FA, and 1 nL of the standards was analyzed by tandem MS (CID) in DDA. The MS-MS/MS data were searched against the mammalian proteome to identify these proteins in confidence
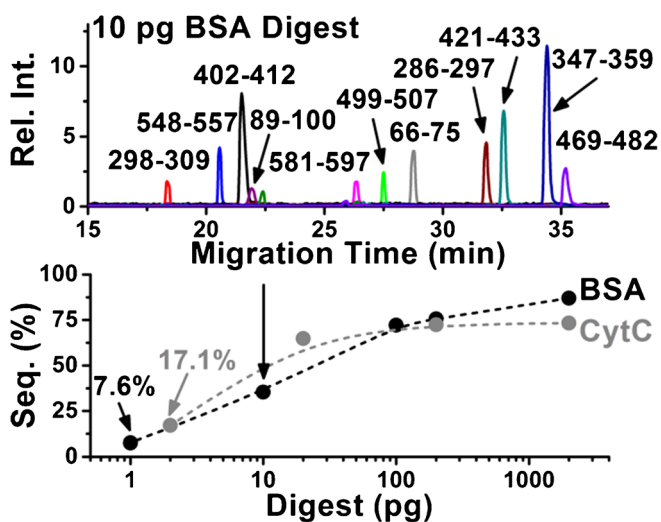

Figure 4. Technology validation for trace-level bottom-up proteomics. Digested bovine serum albumin (BSA) and equine cytochrome *c* (CytC) were serially diluted, and the resulting peptides sequenced by CE-nanoESI-MS using a Qq-TOF. Separation of representative peptides is shown from BSA (**top panel**). Numbers specify amino acid location in the protein sequence. Proteins were identified in confidence (<1% FDR) with a <1 pg lower limit of identification (**bottom panel**), confirming ultrasensitive detection by CE-nanoESI-MS

(<1% FDR, Mascot score >30). Figure 4 exemplifies the separation of select peptides from BSA and identification of the proteins based on the peptide information. The theoretical plate number in the complex BSA digest ranged from a median of ~100,000 to 290,000 (see peptide sequence 499–507), revealing efficient separation performance. As expected, lower protein amounts yielded decreasing sequence coverage. With ~8% sequence coverage, the lower limit of identification was <1 pg for BSA with similar performance for cytochrome *c*. This raises a potential to measure trace amounts of proteins in complex protein digests. We attribute ultrasensitive protein identification by tapered-tip CE-nanoESI to efficient minimization of sample complexity by high-efficiency electrophoretic separation, on-column pre-concentration via field-amplified sample stacking by CE, and efficient and stable ion generation afforded by nanoESI in the cone-jet spraying regime.

CE-nanoESI-MS was applied to limited amounts of protein digests from the posterior half of the mouse cortex. The tissue was isolated, and the proteins were extracted, reduced, alkylated, and digested using a standard bottom-up protocol that was scaled to the total protein content of the sample (see Methods). Digested proteins were suspended to 1 ng/nL in 75% (v/v) ACN containing 0.05% (v/v) AcOH. One ng of digest was analyzed by CE-nanoESI-MS on the Qq-TOF mass spectrometer using DDA. The base peak electropherogram revealed appreciably complex peptide composition despite the limited amount of sample analyzed (Figure 5a). The electropherograms appeared similar between technical replicate measurements (compare top and middle panels). Indeed, the Pearson correlation coefficient (ρ) was 0.99 for 45 randomly chosen peptides, revealing robust performance. These peptides were separated within a relatively short (~20-min) time window (see bottom panel), agreeing with similarly compact separation also noted in other bottom-up proteomic studies by CE [36, 45, 48, 56].

Generated peptide ions were sequenced by tandem MS using DDA. We recently demonstrated that dynamic adjustment of the tandem MS duty cycle depending on precursor ion intensity enhances peptide sequencing during compact electrophoretic separation [56]. Using this strategy, 668 peptide spectral matches (PSMs) were acquired, which identified 407 different peptides, corresponding to ~60% identification rate based on individual MS/MS events. This success rate was enhanced to ~66% by spiking the sheath liquid with 5% (v/v) dimethylsulfoxide, a known supercharging agent [63]. As in nanoLC-nanoESI, supercharging enhanced the quality of tandem mass spectra in CE-nanoESI-MS by promoting the formation of peptides with higher charge states (67% versus 73% of ions doubly charged), which are known to fragment better. These results complement our recent observation for CE-µESI interface, in which supercharging did not appreciably enhance peptide identifications on the same mass spectrometer, likely due to higher flow rates [56]. It follows that peptide identifications appear to increasingly benefit from supercharging in CE-ESI designs that employ low-flow sheath liquid or are sheathless (e.g., [28–32]).
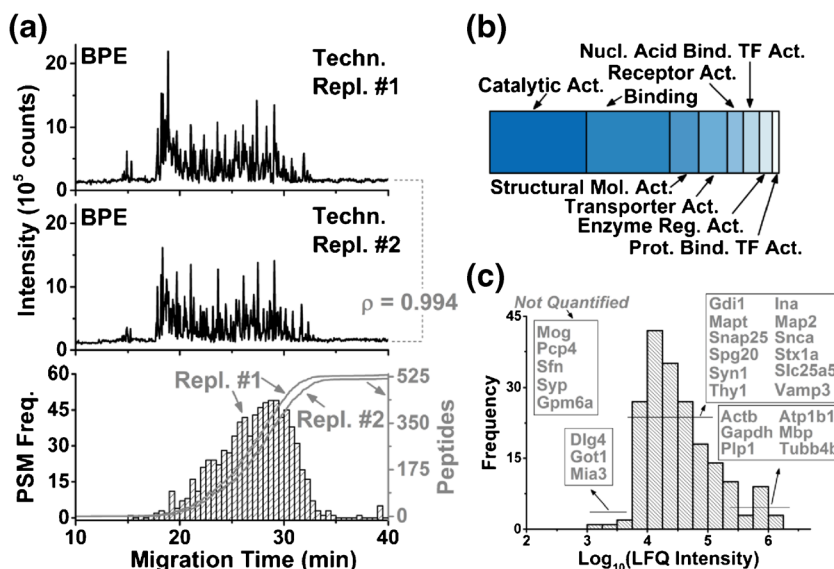
Figure 5. Protein identification from 1 ng protein digest from the mouse cortex. (**a**) Peptide separation was robust, as revealed by a high Pearson correlation (ρ) calculated for 45 randomly selected peptides between technical replicates. Tandem MS enabled rapid acquisition of peptide spectral matches (PSMs) within a ~20-min separation window, identifying ~525 different peptides. Cumulative rate of peptide identification is shown for technical replicates in grey. (**b**) These peptides were mapped to 217 nonredundant protein groups in the encoded mouse proteome (Supplementary Table S1). Gene ontology annotation is shown for these proteins. Key: Act., activity; TF, transcription factor. (**c**) A total of 192 proteins were quantified, which spanned a ~3-log-order concentration range based on calculated label-free quantification (LFQ) intensities. Representative proteins are labeled and grouped into abundance domains (see Supplementary Table S1)

The peptide sequences led to the identification of 217 different protein groups from the 1 ng protein digest from the mouse cortex. PANTHER (Protein Analysis Through Evolutionary Relationships) Gene Ontology annotation suggested that these proteins had structural molecular, catalytic, binding, and transporter activities (Figure 5b). Other categories suggest roles in receptor binding, nucleic acid and protein binding transcription, and enzyme regulation. To estimate the relative abundance of these proteins, we calculated label-free quantification (LFQ) intensities using MaxLFQ [64]. About 12% of the identified proteins were not quantifiable based on the MS/MS data (LFQ intensity = 0). The LFQ intensity values for 192 proteins indicated a ~3-log-order concentration range with tailing toward higher LFQ intensities. Representative proteins are grouped into abundance domains in Figure 5c. A complete list of identified proteins and their calculated LFQ intensity values are in Supplementary Table S1. For example, proteins in the low–middle abundance range included transcription and translation regulators and macromolecular assembly (e.g., Ef1a1, Hspa8), synaptic function (e.g., Dlg4/PSD95, bassoon, and CaMKIIb), and energy production (e.g., Atp9a, Atp5j2). Proteins with high LFQ intensity values were enriched in structural organization (e.g., Tuba1a, Tubb4b, Actb), glycolysis (Gapdh), and myelination (e.g., Mbp, Plp1).

Last, we surveyed the 217 proteins identified by CE-nanoESI-MS based on their known affiliation with neurons, astrocytes, and oligodendrocytes. At least 40 different genes that are commonly used as neuronal markers were readily recognized at the protein level. For example, synaptosomal-associated protein 25 (Snap25), synapsin 1 (Syn1), syntaxin-1a (Stx1a), synaptotagmin 1 (Syt1), vesicle-associated membrane protein 3 (Vamp3/synaptobrevin-3), and GDP dissociation inhibitors 1 and 2 (Gdi1, Gdi2) are implicated in neurotransmitter exocytosis at the synapse [6]. Other proteins such as microtubule-associated protein 2 (Map2) and alpha-internexin (Ina) are neuronal-specific cytoskeletal components. Oligodendrocyte markers include multiple myelin components, such as myelin basic protein (Mbp) and proteolipid protein 1 (Plp1). Finally, key proteins involved in neurodegenerative disorders were detected by our approach. Microtubule-associated protein tau (Mapt) and alpha-synuclein (Snca) accumulate in the brain of patients with Alzheimer's disease, and are mutated in frontotemporal dementia with parkinsonism and Parkinson's disease, respectively [65]. Spartin (Spg20) is mutated in a rare form of hereditary spastic paraplegia [66]. Combined, these results established that CE-nanoESI-MS is able to characterize protein expression in the mammalian brain with sufficient sensitivity to detect markers of healthy and diseased neurons.

Conclusions

Here we developed an ultrasensitive, robust CE-nanoESI interface for MS to enable the discovery characterization of protein translation in 1 ng protein digest from the mouse cortex. This sensitivity raises a potential for detecting proteins expressed by a handful of neurons. The CE-ESI design uses a small-bore

tapered-tip metal emitter to integrate the CE separation capillary into a nanoESI source via a co-axial sheath-flow configuration. We found that the tapered-tip emitter stabilized the Taylor cone with reduced volume in the nano-flow regime (200–350 nL/min), ensuring efficient and robust ion generation within close proximity of the mass spectrometer inlet for maximal ion collection. Combined, these performance metrics provided an estimated 260 zmol lower limit of detection, or 156,000 copies for peptide standards. Compared with other co-axial sheath-flow interfaces, this sensitivity is ~4000-times higher than those based on large-bore emitters [57], ~20–100 times higher than our previous constructs based on small-bore blunt-tip emitters (see earlier and [55, 56]), and is comparable to electrokinetically pumped interfaces using multiple reaction monitoring [43, 44]. While specialized low-flow [45] and sheathless [33] CE-nanoESI interfaces and nanoLC-nanoESI [22, 23] systems recently accomplished 1–10 zmol lower limit of detection, microanalytical tapered-tip CE-nanoESI presents analytical advantages. This interface provides fast analysis time (e.g., ~30 min typical by CE versus ~2–5 h typical by nanoLC), can be constructed with minimal-to-no prior experience in <15 min using readily available commercial components (see Figure 1b), offers robust operation (2 mo tested here without detectable performance deterioration), and compatibility to volume/mass-limited specimens (<1 µL digest deposited here). Combined, these metrics facilitate broad adoptability of the technology for ultrasensitive proteomics also in other laboratories where limited volumes or amounts of protein digests need analysis.

Ultrasensitive peptide detection extends MS-based proteomics to trace amounts of samples. In the work presented here, we demonstrated the identification of 1 pg, or 15 amol of standard proteins. CE-nanoESI enabled the detection of 217 nonredundant protein groups from ~1 ng protein digest from the mouse cortex. In principle, tapered-tip CE-nano-ESI-MS raises sufficient sensitivity to measure hundreds of picograms to few nanograms of proteins contained in small populations of neurons and other single cells. Continuous developments in microscale sampling, protein extraction, and digestion (e.g., by on-column immobilized microreactors [67], fractionation [68], and focused acoustics-assisted sample preparation [23]) can help extend the detectable coverage of the encoded proteome to single cells. To address compact electrophoretic separation, refinements are needed in tandem MS technology. Tandem MS with fast duty cycle using DDA or data-independent acquisition strategies as well as parallelization of MS–MS^n scans using new-generation hybrid instruments promise enhanced protein identifications. Last, besides LFQ as demonstrated here, existing strategies in quantitative proteomics, such as iBAQ, TOP3, TMT, TMT^c, iTRAQ, and SIN, are adaptable to perform relative or absolute quantification on trace amounts of proteins using tapered-tip CE-nanoESI-MS.

Ultrasensitive proteomics raises a potential to understand how differential gene expression coordinates cell heterogeneity during brain development and function. Many of the proteins identified in this work are expressed from genes that are classically used to mark important cell types in the brain: neurons, oligodendrocytes, and astrocytes. We anticipate that the sensitivity of the presented technology is sufficient to identify key proteins involved in different stages of neurodevelopmental or neurodegenerative disease progression in specific brain regions. This approach can lead to a better understanding of the molecular mechanisms underlying disease, to the identification of diagnostic or prognostic biomarkers, or to pinpoint novel therapeutic targets.

Acknowledgment

Compliance with Ethical Standards

Conflict of Interest Disclosure   The authors declare no competing financial interest.

Author Contribution   PN designed the research; MZ and MCM provided the tissue samples and edited the manuscript; PN and SBC analyzed the data and wrote the manuscript.

References

1. Picotti, P., Clement-Ziza, M., Lam, H., Campbell, D.S., Schmidt, A., Deutsch, E.W., Rost, H., Sun, Z., Rinner, O., Reiter, L., Shen, Q., Michaelson, J.J., Frei, A., Alberti, S., Kusebauch, U., Wollscheid, B., Moritz, R.L., Beyer, A., Aebersold, R.: A complete mass-spectrometric map of the yeast proteome applied to quantitative trait analysis. Nature **494**, 266–270 (2013)

2. Nagaraj, N., Kulak, N.A., Cox, J., Neuhauser, N., Mayr, K., Hoerning, O., Vorm, O., Mann, M.: System-wide perturbation analysis with nearly complete coverage of the yeast proteome by single-shot ultra HPLC runs on a bench top Orbitrap. Mol. Cell. Proteom. **11**, M111.013722 (2012)

3. Hebert, A.S., Richards, A.L., Bailey, D.J., Ulbrich, A., Coughlin, E.E., Westphall, M.S., Coon, J.J.: The one hour yeast proteome. Mol. Cell. Proteom. **13**, 339–347 (2014)

4. McAlister, G.C., Nusinow, D.P., Jedrychowski, M.P., Wuhr, M., Huttlin, E.L., Erickson, B.K., Rad, R., Haas, W., Gygi, S.P.: Multinotch MS^3 enables accurate, sensitive, and multiplexed detection of differential expression across cancer cell line proteomes. Anal. Chem. **86**, 7150–7158 (2014)

5. Kim, M.S., Pinto, S.M., Getnet, D., Nirujogi, R.S., Manda, S.S., Chaerkady, R., Madugundu, A.K., Kelkar, D.S., Isserlin, R., Jain, S., Thomas, J.K., Muthusamy, B., Leal-Rojas, P., Kumar, P., Sahasrabuddhe, N.A., Balakrishnan, L., Advani, J., George, B., Renuse, S., Selvan, L.D.N., Patil, A.H., Nanjappa, V., Radhakrishnan, A., Prasad, S., Subbannayya, T., Raju, R., Kumar, M., Sreenivasamurthy, S.K., Marimuthu, A., Sathe, G.J., Chavan, S., Datta, K.K., Subbannayya, Y., Sahu, A., Yelamanchi, S.D., Jayaram, S., Rajagopalan, P., Sharma, J., Murthy, K.R., Syed, N., Goel, R., Khan, A.A., Ahmad, S., Dey, G.,

Mudgal, K., Chatterjee, A., Huang, T.C., Zhong, J., Wu, X.Y., Shaw, P.G., Freed, D., Zahari, M.S., Mukherjee, K.K., Shankar, S., Mahadevan, A., Lam, H., Mitchell, C.J., Shankar, S.K., Satishchandra, P., Schroeder, J.T., Sirdeshmukh, R., Maitra, A., Leach, S.D., Drake, C.G., Halushka, M.K., Prasad, T.S.K., Hruban, R.H., Kerr, C.L., Bader, G.D., Iacobuzio-Donahue, C.A., Gowda, H., Pandey, A.: A draft map of the human proteome. Nature **509**, 575–581 (2014)

6. Sharma, K., Schmitt, S., Bergner, C.G., Tyanova, S., Kannaiyan, N., Manrique-Hoyos, N., Kongi, K., Cantuti, L., Hanisch, U.K., Philips, M.A., Rossner, M.J., Mann, M., Simons, M. Cell type- and brain region-resolved mouse brain proteome. Nat. Neurosci. **18**, 1819–1831 (2015)

7. Tasic, B., Menon, V., Nguyen, T.N., Kim, T.K., Jarsky, T., Yao, Z.Z., Levi, B., Gray, L.T., Sorensen, S.A., Dolbeare, T., Bertagnolli, D., Goldy, J., Shapovalova, N., Parry, S., Lee, C., Smith, K., Bernard, A., Madisen, L., Sunkin, S.M., Hawrylycz, M., Koch, C., Zeng, H.K.: Adult mouse cortical cell taxonomy revealed by single cell transcriptomics. Nat. Neurosci. **19**, 335–346 (2016)

8. Zeisel, A., Munoz-Manchado, A.B., Codeluppi, S., Lonnerberg, P., La Manno, G., Jureus, A., Marques, S., Munguba, H., He, L.Q., Betsholtz, C., Rolny, C., Castelo-Branco, G., Hjerling-Leffler, J., Linnarsson, S.: Cell types in the mouse cortex and hippocampus revealed by single-cell RNA-Seq. Science **347**, 1138–1142 (2015)

9. Lanni, E.J., Rubakhin, S.S., Sweedler, J.V.: Mass spectrometry imaging and profiling of single cells. J. Proteom. **75**, 5036–5051 (2012)

10. Rubakhin, S.S., Romanova, E.V., Nemes, P., Sweedler, J.V.: Profiling metabolites and peptides in single cells. Nat. Methods **8**, S20–S29 (2011)

11. Buchberger, A., Yu, Q., Li, L.J.: Advances in mass spectrometric tools for probing neuropeptides. Annu. Rev. Anal. Chem. **8**, 485–509 (2015)

12. Wang, D.J., Bodovitz, S.: Single cell analysis: the new frontier in 'omics. Trends Biotechnol. **28**, 281–290 (2010)

13. Hofstadler, S.A., Swanek, F.D., Gale, D.C., Ewing, A.G., Smith, R.D.: Capillary electrophoresis electrospray ionization Fourier transform ion cyclotron resonance mass spectrometry for direct analysis of cellular proteins. Anal. Chem. **67**, 1477–1480 (1995)

14. Valaskovic, G.A., Kelleher, N.L., McLafferty, F.W.: Attomole protein characterization by capillary electrophoresis-mass spectrometry. Science **273**, 1199–1202 (1996)

15. Mellors, J.S., Jorabchi, K., Smith, L.M., Ramsey, J.M.: Integrated microfluidic device for automated single cell analysis using electrophoretic separation and electrospray ionization mass spectrometry. Anal. Chem. **82**, 967–973 (2010)

16. Bendall, S.C., Simonds, E.F., Qiu, P., Amir, E.A.D., Krutzik, P.O., Finck, R., Bruggner, R.V., Melamed, R., Trejo, A., Ornatsky, O.I., Balderas, R.S., Plevritis, S.K., Sachs, K., Pe'er, D., Tanner, S.D., Nolan, G.P.: Single-cell mass cytometry of differential immune and drug responses across a human hematopoietic continuum. Science **332**, 687–696 (2011)

17. Waanders, L.F., Chwalek, K., Monetti, M., Kumar, C., Lammert, E., Mann, M.: Quantitative proteomic analysis of single pancreatic islets. Proc. Natl. Acad. Sci. USA **106**, 18902–18907 (2009)

18. Wang, N., Xu, M.G., Wang, P., Li, L.: Development of mass spectrometry-based shotgun method for proteome analysis of 500 to 5000 cancer cells. Anal. Chem. **82**, 2262–2271 (2010)

19. Chen, Q., Yan, G.Q., Gao, M.X., Zhang, X.M.: Direct digestion of proteins in living cells into peptides for proteomic analysis. Anal. Bioanal. Chem. **407**, 1027–1032 (2015)

20. Yue, G.H., Luo, Q.Z., Zhang, J., Wu, S.L., Karger, B.L.: Ultratrace LC/MS proteomic analysis using 10-μm-i.d. porous layer open tubular poly(-styrene-divinylbenzene) capillary columns. Anal. Chem. **79**, 938–946 (2007)

21. Luo, Q., Yue, G., Valaskovic, G.A., Gu, Y., Wu, S.L., Karger, B.L.: On-Line line 1D and 2D porous layer open tubular/LC-ESI-MS using 10-μm-i.d. poly(styrene-divinylbenzene) columns for ultrasensitive proteomic analysis. Anal. Chem. **79**, 6174–6181 (2007)

22. Shen, Y., Tolic, N., Masselon, C., Pasa-Tolic, L., Camp, D.G., Hixson, K.K., Zhao, R., Anderson, G.A., Smith, R.D.: Ultrasensitive proteomics using high-efficiency on-line micro-SPE-nanoLC-nanoESI MS and MS/MS. Anal. Chem. **76**, 144–154 (2004)

23. Li, S.Y., Plouffe, B.D., Belov, A.M., Ray, S., Wang, X.Z., Murthy, S.K., Karger, B.L., Ivanov, A.R.: An integrated platform for isolation, processing, and mass spectrometry-based proteomic profiling of rare cells in whole blood. Mol. Cell. Proteom. **14**, 1672–1683 (2015)

24. Smith, R.D., Barinaga, C.J., Udseth, H.R.: Improved electrospray ionization interface for capillary zone electrophoresis-mass spectrometry. Anal. Chem. **60**, 1948–1952 (1988)

25. Bonvin, G., Schappler, J., Rudaz, S.: Capillary electrophoresis-electrospray ionization-mass spectrometry interfaces: fundamental concepts and technical developments. J. Chromatogr. A. **1267**(17–31), 36 (2012)

26. Lindenburg, P.W., Haselberg, R., Rozing, G., Ramautar, R.: Developments in interfacing designs for CE-MS: towards enabling tools for proteomics and metabolomics. Chromatographia **78**, 367–377 (2015)

27. Maxwell, E.J., Chen, D.D.Y.: Twenty years of interface development for capillary electrophoresis-electrospray ionization-mass spectrometry. Anal. Chim. Acta **627**, 25–33 (2008)

28. Bendahl, L., Hansen, S.H., Olsen, J.: A new sheathless electrospray interface for coupling of capillary electrophoresis to ion-trap mass spectrometry. Rapid Commun. Mass Spectrom. **16**, 2333–2340 (2002)

29. Chen, Y.R., Her, G.R.: A simple method for fabrication of silver-coated sheathless electrospray emitters. Rapid Commun. Mass Spectrom. **17**, 437–441 (2003)

30. Ramsey, R.S., McLuckey, S.A.: Capillary electrophoresis/electrospray ionization ion trap mass spectrometry using a sheathless interface. J. Microcolumn Sep. **7**, 461–469 (1995)

31. Zamfir, A.D., Dinca, N., Sisu, E., Peter-Katalinic, J.: Copper-coated microsprayer interface for on-line sheathless capillary electrophoresis electrospray mass spectrometry of carbohydrates. J. Sep. Sci. **29**, 414–422 (2006)

32. Kriger, M.S., Cook, K.D., Ramsey, R.S.: Durable gold-coated fused silica capillaries for use in electrospray mass spectrometry. Anal. Chem. **67**, 385–389 (1995)

33. Moini, M.: Simplifying CE-MS Operation. 2. Interfacing low-flow separation techniques to mass spectrometry using a porous tip. Anal. Chem. **79**, 4241–4246 (2007)

34. Faserl, K., Sarg, B., Kremser, L., Lindner, H.: Optimization and evaluation of a sheathless capillary electrophoresis-electrospray ionization mass spectrometry platform 37 for peptide analysis: comparison to liquid chromatography electrospray ionization mass spectrometry. Anal. Chem. **83**, 7297–7305 (2011)

35. Wang, C.C., Lee, C.S., Smith, R.D., Tang, K.Q.: Capillary isotachophoresis-nanoelectrospray ionization-selected reaction monitoring MS via a novel sheathless interface for high sensitivity sample quantification. Anal. Chem. **85**, 7308–7315 (2013)

36. Wang, Y., Fonslow, B.R., Wong, C.C.L., Nakorchevsky, A., Yates, J.R.: Improving the comprehensiveness and sensitivity of sheathless capillary electrophoresis-tandem mass spectrometry for proteomic analysis. Anal. Chem. **84**, 8505–8513 (2012)

37. Guo, X.J., Fillmore, T.L., Gao, Y.Q., Tang, K.Q.: Capillary electrophoresis-nanoelectrospray ionization selected reaction monitoring mass spectrometry via a true sheathless metal-coated emitter interface for robust and high-sensitivity sample quantification. Anal. Chem. **88**, 4418–4425 (2016)

38. Han, X., Wang, Y., Aslanian, A., Bern, M., Lavallee-Adam, M., Yates, J.R.: Sheathless capillary electrophoresis tandem mass spectrometry for top-down characterization of *Pyrococcus furiosus* proteins on a proteome scale. Anal. Chem. **86**, 11006–11012 (2014)

39. Zhao, Y.M., Riley, N.M., Sun, L.L., Hebert, A.S., Yan, X.J., Westphall, M.S., Rush, M.J.P., Zhu, G.J., Champion, M.M., Medie, F.M., Champion, P.A.D., Coon, J.J., Dovichi, N.J.: Coupling capillary zone electrophoresis with electron transfer dissociation and activated ion electron transfer dissociation for top-down proteomics. Anal. Chem. **87**, 5422–5429 (2015)

40. Bush, D.R., Zang, L., Belov, A.M., Ivanov, A.R., Kargert, B.L.: High-resolution CZE-MS quantitative characterization of intact biopharmaceutical proteins: proteoforms of interferon-β1. Anal. Chem. **88**, 1138–1146 (2016)

41. Bruins, A.P., Covey, T.R., Henion, J.D.: Ion spray interface for combined liquid chromatography/atmospheric pressure ionization mass spectrometry. Anal. Chem. **59**, 2642–2646 (1987)

42. Hashimoto, M., Ishihama, Y., Tomita, M., Soga, T.: Microelectrospray interface with coaxial sheath flow for high-resolution capillary electrophoresis/mass spectrometry separation. Rapid Commun. Mass Spectrom. **21**, 3579–3584 (2007)

43. Sun, L.L., Li, Y.H., Champion, M.M., Zhu, G.J., Wojcik, R., Dovichi, N.J.: Capillary zone electrophoresis-multiple reaction monitoring from 100 pg of RAW 264.7 cell lysate digest. Analyst **138**, 3181–3188 (2013)

44. Li, Y.H., Wojcik, R., Dovichi, N.J., Champion, M.M.: Quantitative multiple reaction monitoring of peptide abundance introduced via a capillary zone electrophoresis-electrospray interface. Anal. Chem. **84**, 6116–6121 (2012)

45. Sun, L., Zhu, G., Zhao, Y., Yan, X., Mou, S., Dovichi, N.J.: Ultrasensitive and fast bottom-up analysis of femtogram amounts of complex proteome digests. Angew. Chem. Int. Ed. **52**, 13661–13664 (2013)

46. Li, Y.H., Compton, P.D., Tran, J.C., Ntai, I., Kelleher, N.L.: Optimizing capillary electrophoresis for top-down proteomics of 30–80 kDa proteins. Proteomics **14**, 1158–1164 (2014)

47. Sun, L.L., Zhu, G.J., Zhang, Z.B., Mou, S., Dovichi, N.J.: Third-generation electrokinetically pumped sheath-flow nanospray interface with improved stability and sensitivity for automated capillary zone electrophoresis-mass spectrometry analysis of complex proteome digests. J. Proteome Res. **14**, 2312–2321 (2015)

48. Ludwig, K.R., Sun, L.L., Zhu, G.J., Dovichi, N.J., Hummon, A.B.: Over 2300 phosphorylated peptide identifications with single-shot capillary zone electrophoresis tandem mass spectrometry in a 100 min separation. Anal. Chem. **87**, 9532–9537 (2015)

49. Lapainis, T., Rubakhin, S.S., Sweedler, J.V.: Capillary electrophoresis with electrospray ionization mass spectrometric detection for single-cell metabolomics. Anal. Chem. **81**, 5858–5864 (2009)

50. Nemes, P., Knolhoff, A.M., Rubakhin, S.S., Sweedler, J.V.: Metabolic differentiation of neuronal phenotypes by single-cell capillary electrophoresis-electrospray ionization mass spectrometry. Anal. Chem. **83**, 6810–6817 (2011)

51. Nemes, P., Rubakhin, S.S., Aerts, J.T., Sweedler, J.V.: Qualitative and quantitative metabolomic investigation of single neurons by capillary electrophoresis electrospray ionization mass spectrometry. Nat. Protoc. **8**, 783–799 (2013)

52. Nemes, P., Knolhoff, A.M., Rubakhin, S.S., Sweedler, J.V.: Single-cell metabolomics: changes in the metabolome of freshly isolated and cultured neurons. ACS Chem. Neurosci. **3**, 782–792 (2012)

53. Onjiko, R.M., Moody, S.A., Nemes, P.: Single-cell mass spectrometry reveals small molecules that affect cell fates in the 16-cell embryo. Proc. Natl. Acad. Sci. USA **112**, 6545–6550 (2015)

54. Onjiko, R.M., Morris, S.E., Moody, S.A., Nemes, P.: Single-cell mass spectrometry with multi-solvent extraction identifies metabolic differences between left and right blastomeres in the 8-cell frog (*Xenopus*) embryo. Analyst **141**, 3648–3656 (2016)

55. Lombard-Banek, C., Moody, S.A., Nemes, P.: Single-cell mass spectrometry for discovery proteomics: quantifying translational cell heterogeneity in the 16-cell frog (*Xenopus*) embryo. Angew. Chem. Int. Ed. **55**, 2454–2458 (2016)

56. Lombard-Banek, C., Reddy, S., Moody, S.A., Nemes, P.: Label-free quantification of proteins in single embryonic cells with neural fate in the cleavage-stage frog (*Xenopus laevis*) embryo using capillary electrophoresis electrospray ionization high-resolution mass spectrometry (CE-ESI-HRMS). Mol. Cell. Proteom. **15**, 2756–2768 (2016)

57. Gonzalez-Ruiz, V., Codesido, S., Far, J., Rudaz, S., Schappler, J.: Evaluation of a new low sheath-flow interface for CE-MS. Electrophoresis **37**, 936–946 (2016)

58. Craig, R., Cortens, J.P., Beavis, R.C.: Open source system for analyzing, validating, and storing protein identification data. J. Proteome. Res. **3**, 1234–1242 (2004)

59. Smith, R.D., Olivares, J.A., Nguyen, N.T., Udseth, H.R.: Capillary zone electrophoresis-mass spectrometry using an electrospray ionization interface. Anal. Chem. **60**, 436–441 (1988)

60. Schmidt, A., Karas, M., Dulcks, T.: Effect of different solution flow rates on analyte ion signals in nano-ESI MS, or: When does ESI turn into nano-ESI? J. Am. Soc. Mass Spectrom. **14**, 492–500 (2003)

61. Nemes, P., Marginean, I., Vertes, A.: Spraying mode effect on droplet formation and ion chemistry in electrosprays. Anal. Chem. **79**, 3105–3116 (2007)

62. Valaskovic, G.A., Murphy, J.P., Lee, M.S.: Automated orthogonal control system for electrospray ionization. J. Am. Soc. Mass Spectrom. **15**, 1201–1215 (2004)

63. Iavarone, A.T., Williams, E.R.: Mechanism of charging and supercharging molecules in electrospray ionization. J. Am. Chem. Soc. **125**, 2319–2327 (2003)

64. Cox, J., Hein, M.Y., Luber, C.A., Paron, I., Nagaraj, N., Mann, M.: Accurate proteome-wide label-free quantification by delayed normalization and maximal peptide ratio extraction, termed MaxLFQ. Mol. Cell. Proteom. **13**, 2513–2526 (2014)

65. Ferencz, B., Gerritsen, L.: Genetics and underlying pathology of dementia. Neuropsychol. Rev. **25**, 113–124 (2015)

66. Manzini, M.C., Rajab, A., Maynard, T.M., Mochida, G.H., Tan, W.H., Nasir, R., Hill, R.S., Gleason, D., Al Saffar, M., Partlow, J.N., Barry, B.J., Vernon, M., LaMantia, A.S., Walsh, C.A.: Developmental and degenerative features in a complicated spastic paraplegia. Ann. Neurol. **67**, 516–525 (2010)

67. Sun, L.L., Zhu, G.J., Dovichi, N.J.: Integrated capillary zone electrophoresis electrospray ionization tandem mass spectrometry system with an immobilized trypsin microreactor for online digestion and analysis of picogram amounts of RAW 264.7 cell lysate. Anal. Chem. **85**, 4187–4194 (2013)

68. Faserl, K., Kremser, L., Muller, M., Teis, D., Lindner, H.H.: Quantitative proteomics using ultra low flow capillary electrophoresis-mass spectrometry. Anal. Chem. **87**, 4633–4640 (2015)

69. Vizcaíno, J., Csordas, A., del Toro, N., Dianes, J., Griss, J., Lavidas, I., Mayer, G., Perez-Riverol, Y., Reisinger, F., Ternent, T., Xu, Q., Wang, R., Hermjakob, H.: Update of the PRIDE database and related tools. Nucleic. Acids. Res. **44**, D447–D456 (2016)